DELETERIOUS ALKALI-AGGREGATE REACTION IN CONCRETE: RELATIONSHIP BETWEEN MINERALOGICAL AND MICROSTRUCTURAL CHARACTERISTICS OF AGGREGATES VERSUS EXPANSION TESTS

Nélia Castro[1,*], Børge J. Wigum[1], Maarten A.T.M. Broekmans[2]

[1]Norwegian University of Science and Technology (NTNU),
Department of Geology and Minerals Resources Engineering, TRONDHEIM, Norway

[2]Geological Survey of Norway, Dept. of Industrial Minerals and Metals,
TRONDHEIM, Norway

Abstract

A variety of aggregate materials from European sources have been studied in the EU-funded PARTNER project in 2002-2006 to evaluate the suitability of different European test methods. It was found that petrography can potentially provide effective and reliable results quickly than other method, but with some limitations [1].

This study uses available post-mortem expansion-test specimen and virgin aggregate from PARTNER, for mineralogical and microstructural characterization of reactive constituents. This contribution reports initial results from characterization of the silica minerals in different aggregate materials, using a range of techniques including optical petrography, image analysis, and XRD. When compared with expansion testing results, these findings will strengthen our understanding of the AAR mechanism. Ultimately, this contribution can provide the basis for a proposal to improve the reliability and accuracy of the petrographic test procedure and contribute to a better understanding of the expansion tests.

¶

Keywords: ASR, aggregates for concrete, petrography, image analysis, XRD

1 INTRODUCTION

This paper presents the initial results from microstructural and mineralogical characterization of concrete aggregates in post-mortem expansion test specimen and virgin aggregate from the PARTNER project [1]. This study is part of a project that rose from the interest of applying geology knowledge and techniques to the study of the properties and qualities of the silica minerals that contribute to the alkali-reactivity of the aggregates for concrete. The aim of the project is to study the relationship between aggregate petrological properties and expansion test results. Mineralogical, geochemical and microstructural characteristics of silica minerals in aggregate, with focus on the properties and qualities of silica minerals that can contribute to its dissolution under 'alkali silica reaction (ASR) conditions', will be investigated. Results from expansion testing will provide a better knowledge of aggregate properties and performance in concrete and consequently a better understanding of the ASR mechanism. Full theoretical understanding on this very complex field is beyond the scope of this project. However, the findings of the project are intended to provide suggestions to the introduction of quantitative parameters in the petrographic test method, which can

* Correspondence to: nelia.castro@ntnu.no

improve the accuracy and reproducibility of the petrographic test procedure (RILEM AAR-1 [2]) and contribute to a better understanding of the expansion tests.

Though the exact mechanism of ASR is a matter of dispute, there is general consensus that at some point the mechanism involves silica dissolution. A range of properties and qualities are known to affect the dissolution of quartz under geological conditions, and some may apply to 'ASR conditions' at pH14 and ambient temperature. Some quartz properties are relatively easy to assess, others require more specialized instrumentation or equipment. A summary of some fundamental considerations with respect to the solubility of silica minerals under geological and under ASR conditions can be found in Broekmans [3, 4].

Test methods to assess the ASR-potential of aggregate for use in concrete have been under development for several decades. However, none of the accepted current methods actually assess aggregate properties in terms of 'quartz solubility under ASR conditions'. In nearly all tests, aggregate is exposed to severe conditions (eg. 1N NaOH, 38-60-80°C and up) to provoke expansion within acceptable time (i.e. weeks) for the building and construction industry.

Different European test methods were evaluated for their suitability for use with the wide variety of aggregates found across Europe in the EU-funded PARTNER project in 2002-2006. The project had 24 partners from 14 countries assessing 22 different types of aggregates from 10 countries in an overall total of 413 tests, comprising expansion testing and rock classification using thin section petrography. Final results have been published in [1, 5, 6], and references therein. The overall conclusion from PARTNER is that the RILEM AAR- 2 [7] and AAR-4 [8] test are able to reliably identify the reactivity of normally and non-reactive aggregates. However, slowly aggregates typically require an extended test period.

Petrographic assessment according to the protocol described in RILEM AAR-1 [2] classifies concrete aggregate as potentially reactive or innocuous based on rock nomenclature. This procedure does not assess the actual amount of individual potentially reactive mineral constituents in an aggregate particle, but rather quantifies rock types that have been identified as deleterious in field structures. On a worldwide basis, petrographers use essentially the same procedures for thin section preparation, and the same type of instrumentation to study them. However, different schools exist on the 'correct' application of rock nomenclature complicating use of uniform terminology (see eg. discussion in [9]). On top of that comes inter-operator variation due to variable levels of experience and skill. In addition, the alkali-reactivity potential of a given rock type is known to vary from one location (region, nation) to another, which has resulted in rather different rock classifications reflecting local experience [1, 10]. Together, above issues effectively prevent simple uniform classification of a given lithology as 'always alkali-reactive' or 'invariably innocuous', rendering petrographic assessment more complicated than desirable.

Here, we have investigated normally, slowly and non-reactive rock types in post-mortem concrete prisms and mortar bars previously tested for expansion in PARTNER, in addition to their untested virgin counterparts originally stocked for reference. This enables direct comparison of changes brought about by the reaction as well identification of certain properties/qualities that render the quartz in a given lithology alkali-reactive or innocuous. Materials were initially assessed by thin section petrography to identify actually alkali-reactive aggregate particles. Subsequently, selected particles investigated using digital image analysis and X-ray powder diffraction to assess mineral content.

2 MATERIALS AND METHODS

2.1 Materials

This study uses available post-mortem expansion-test specimen and virgin aggregate from the PARTNER project, for mineralogical and microstructural characterization of reactive constituents. In total, 22 post-mortem expansion test concrete prisms and 3 virgin aggregate samples were available for

characterization, representing 14 different aggregate types from 8 different European countries, including 6 normally, 3 slowly, and 5 non-reactive aggregates cf. RILEM AAR-1 [2] classification. In total, 13 combinations of aggregates were tested in the 22 prisms: 3 combinations with the AAR-3 method [11], 12 combinations with the AAR-4 method [8] and 7 combinations with the German method [12]. Further details are described in [13].

All post-mortem expansion-test specimen and virgin aggregate were investigated by petrography. The main focus was given to the identification of potentially reactive particles of aggregate that could be suitable to further characterization by analytical techniques of petrography and mineralogy.

Three aggregates (It2, N4, and N5) were selected for grain size analysis of quartz by thin section petrography of post-mortem expansion-test specimens and virgin aggregate, all initially classified as slowly reactive (Table 1). The alkali-reactivity of quartz bearing rock types is usually attributed to the presence of strained, microscrystalline or cryptocrystalline quartz. A number of methods have been suggested to correlate aggregate microstructure with the expansion observed in concrete. Wigum [14]found a correlation between expansion behavior of a number of mylonites, granite and gneiss rocks versus 1) the inverse of the mean grain size d_{50}, and 2) the total grain boundary area of quartz. Wigum *et al.* [15] analysed additional samples of different rock types confirming his earlier observations. In this study, the grain size analysis follows the same procedures developed by Wigum [14] but uses image analyses instead of point-counting.

It is generally accepted that the alkali-reactivity of flint/chert and silicified limestones is related to the presence of amorphous or poorly-crystalline forms of silica, eg. opal, chalcedony and possibly also moganite. Though different silica polymorphs do have different solubilities, the most relevant polymorph present in the vast majority of concrete aggregates is α-SiO_2 or ordinary low-quartz, with subordinate quantities of chalcedony and/or opaline silica in certain lithologies [3, 4]. The lattice quality of the quartz plays an important role in determining its alkali-reactivity potential, a highly disordered structure being assumed more reactive than quartz-proper [16]. On the other hand, laboratory experiments investigating dissolution of natural quartzes with a broad range of dislocation densities were unable to reveal any measurable differences [17]. In this study, four aggregates (B1, D1, G1 – normally reactive, F1 – non-reactive; see Table 2) were assessed by X-ray diffraction (XRD) to identify silica polymorphs other than quartz.

2.2 Methods for assessment and analysis

Petrography

All post-mortem expansion-test specimen and virgin aggregate were investigated by petrography. Two sections ~20mm thick were cut lengthwise from each concrete prism with a 3mm thick diamond blade. One section was impregnated with fluorescent epoxy and polished according to Danish standard DS 423.39 [18], the other section was left unprepared. Both sections were studied in a Leitz-Wild Heerbrugg stereomicroscope using incident plain or fluorescent illumination to identify AAR reaction products and reactive aggregate particles. Subsequently, fluorescence-impregnated polished thin sections comprising confirmed alkali-reactive particles were prepared from the unprepared section using the procedure outlined in Danish Standard DS 423.40 [19] with minor adaptations. Due to the thickness of the diamond blade, a >3mm mismatch exists between fluorescent versus unprepared plane sections, and the thin section prepared from latter, with possible consequences for intra-particle variation in mineral content and texture/fabric.

Virgin aggregate material was weighed and washed using ordinary tap water. Particles were counted and separated manually per lithology using a Leitz-Wild Heerbrugg stereomicroscope. Polished thin sections of potentially alkali-reactive lithologies as well as some unidentified particles were prepared using standard procedures (e.g. [20]). Thin sections were analysed in a Nikon Eclipse E600 microscope using transmitted

illumination in plane-polarized light (PPL), cross-polarized light (XPL), and incident fluorescent illumination (FL), as applicable.

Grain size analysis of quartz

Three aggregates (It2, N4, and N5 – all slowly reactive) were selected for grain size analysis of quartz by post-mortem thin section petrography of expansion test concrete prisms and matching virgin aggregate particles. Potentially reactive particles identified include gneiss, rhyolite, granite, cataclasite, greywacke, and quartzite (Table 1). The grain size analysis comprises the same type of assessment as described in [14], but uses automated image analysis instead of manual point counting. Re-assessment of the original thin sections from [14] by automated analysis produced results within analytical error, but significantly faster [21].

The Lazy Grain Boundary (LGB) method [22, 23] was used to create grain boundary maps of the quartz contained in the selected aggregates. The LGB method is based on a set of macro commands programmed for Image SXM [24]. The procedure makes use of multiple input images. Sets of input images composed of six micrographs with crossed polarizers and λ-plate rotated 0-150° at 30° increments were acquired in a Leica DM 2500P polarizing microscope with a Jenoptik ProgRes digital camera system. For reliable analysis, the image set must comprise a statistically sufficient number of grains, which is again a combined function of microscope magnification, grain size, and rock heterogeneity. The majority of the image sets were processed fully automated by the LGB method, a few required additional minor manual correction, eg. repairing discontinuous grain boundaries and/or erasing pending relics. After completed segmentation, grains were digitally analyzed for major and minor axis length, area and perimeter. Numerical data were collated in a spreadsheet for further processing.

The examination of a rock under a microscope gives a two-dimensional image and there are a number of measurements that can be made in order to characterize it grains size. In point-counting studies, usually the maximum grain length is measured and used as the diameter. In this case, is considered that the grain is a sphere (equivalent) of this maximum dimension. When using image analysis, other quantity such as minimum length, volume or area can be used; however, will produce a different result for the grain size. Each answer will be correct, giving a true result for the property being measured. Independently of the method used to make the measurements (point-counting or image analysis) it is important to keep in mind a basic principle of stereology: a two-dimensional image will produce an overestimation of small grain sizes. Heilbronner and Bruhn [25] showed that the volume weighted distribution of radii of spheres, V(R), conveys more physically relevant information than the numerical distribution of radii of sectional circles, h(r), when it comes to grain size analysis. On other words, it corrects for the typical overestimation of small grains. In the present work, the areas of the grains measured by image analysis were used to calculate the equivalent circle diameter (d_A), which means that the grain size is defined as the diameter of a circle having the same area. The equivalent circle diameters were then grouped into histograms of 20 classes, where the bins are delimited by their upper bound. The program StripStar [26] was used to calculate the parent distributions of spheres from the histograms of equivalent circle diameters; or in other words to calculate the equivalent spherical diameter (d_V). In this case the grain size is defined as the diameter of a sphere having the same volume.

The mean grain size of quartz and the total grain boundary area of quartz, calculated using d_V as grain size, were used as size descriptors in this work. These descriptors were calculated following the same assumptions of Wigum [14] with minor changes. For determination of the mean grain size of quartz, the d_{50} (mm) read from the cumulative grain size distribution curve was used. In order to estimate the total grain boundary area of quartz, each grain, including subgrains, was assumed to be spherical in shape. The average grain size between two selected fractions was used to calculate the specific surface area (*SS*) for this specific part of the grading. The specific surface area obtained was multiplied by the amount of grains in that fraction

(*f*). This was done for all the selected fractions in the grading and all results summed up in order to obtain the grain boundary area for the entire grading. The total amount of quartz in the rock ($Q_{\%}$) was obtained by a visual estimation from the thin-section using volume % estimation diagrams. By multiplying the grain boundary area with the total amount of quartz in the rock an estimate for the total grain boundary area of quartz (m^2/cm^3) in each sample was obtained. Additional details about the grain size analysis of quartz by image analysis are elaborated in [21].

X-ray diffraction (XRD)

Four aggregates (B1, D1, G1 – normally reactive, F1 – slowly reactive) were selected for mineralogical characterization by XRD. A total of 10 aggregate particles were analyzed with emphasis on identification and quantification of silica polymorphs. Potentially reactive lithologies identified by thin section petrography include flint/chert and siliceous limestone (Table 2).

Castro et al. [27] compared XRD analyses in polished and powdered specimen prepared from the same single aggregate particle and demonstrated that, for fine-grained rocks without preferred orientation like eg. chert, diffraction results are within analytical error. As an advantage, polished sections can also be used for petrography using reflected light (standard 30μm thin sections are ***not*** recommended for XRD), and for subsequent in-situ chemical analysis by EMPA or SEM-EDS. Thus, this study uses polished specimens.

Ten aggregate particles were selected for XRD analysis by prior post-mortem thin section petrography on expansion test concrete prisms and matching virgin particles. The particles were cut from the unprepared counterparts, plane polished with 0.25μm diamond, and mounted on a PMMA holder using pressure-sensitive adhesive. In the instrument, specimen height was carefully adjusted to the focal point of the goniometer to minimize offset and error in the apparent diffraction angle.

Operating conditions of the Bruker D8 Advance X-ray diffractometer were set to 40kV and 40mA, using Ni-filtered CuKα radiation of wavelength λ=1.54178Å. Specimen were analyzed spinning. Diffractograms were recorded from 2-80° 2θ, in 0.01° 2θ increments with 1s counting time per increment, with total scan time 2h10m. Phase quantification was performed using the Rietveld refinement software TOPAS 4.0 with the fundamental parameter approach. Resulting detection limits are on the order of ~1vol%, depending on eg. bulk mineral modal content, intergrinding effects, (cryptic) preferred orientation, all as applicable.

3 RESULTS

Petrography

Thin section petrography confirms the presence of two different groups of potentially alkali-reactive rocks in the materials studied. The first group comprises slowly-reactive rock types, like gneiss, rhyolite, granite, cataclasite, greywacke, and quartzite, which were further assessed by grain size analysis of quartz. The cataclastic rock of granitic composition in aggregate N4 shows extensive geo-tectonic deformation leading to faulting and post-tectonic compaction of debris and cementation by redeposition and recrystallization. In contrast, the quartzite of N5 and gneiss of It2 both show limited deformation and recrystallization only.

The second group comprises normally reactive flint/chert and silicified limestone, which were further investigated by XRD to identify and quantify silica polymorphs. Additional details from thin section petrography are elaborated in [13].

Grain size analysis of quartz

Results from image analysis and data post-processing are collated in Table 3. The number of individual quartz grains assessed by the LGB method ranges from 13061 to 27606, whereas traditional point-

counting petrography typically assesses ~200 grains. The time needed to process a single sample varied from 30 to 120 minutes, in contrast to non-automated assessment requiring up to a whole day for a single thin section.

Furthermore, the cataclasite of N4 has a greater inverse mean grain size $1/d_{50}$ than the less deformed quartzite in N5 and gneiss in It2, and consequently a larger total grain boundary area than both other lithologies.

X-ray diffraction (XRD)

Initial results from the XRD analysis, for selected particles, are normalized to 100vol% and are presented in Table 4 together with rock names from petrographic assessment. Main rock-forming constituents are quartz and calcite. Dolomite content in BI-13, as well as calcite contents in F1-40, F1-41 and F1-43 are all very near the lower limit of detection at ~1vol%, hence are of indicative value only. Materials D1-01 and D1-05 consisting of opaline silica in a limestone host, appear to contain a substantial volume of light silica polymorphs cristobalite and tridymite, presumably representing opal-CT.

4 DISCUSSION

A first assessment by detailed petrography was essential to identify reactive aggregate particles and select the properties and qualities of silica minerals that can contribute to it dissolution in "ASR-environment" relevant to investigate in the scope of the project. Original descriptions elaborated during the PARTNER project have been limited to a few lines in the final PARTNER report, and therefore important information essential to the present work was lacking.

The results of detailed petrography and grain size analysis of quartz by image analysis are consistent with each other. The sample with higher degree of deformation, like N4, have a larger total grain boundary area of quartz than rocks that enjoyed less extensive deformation, such as samples N5 and It2. With image analysis not only is it possible to analyse samples much faster than with point-counting, a much larger number of grains can be analysed. Furthermore, typical stereological problems such as the overestimation of the small grains produced by a two-dimension representation of a rock (thin-section) can be easily and efficiently overcome. The calculated values of the inverse of the mean grain size of quartz and the total grain boundary of quartz were compared with expansion tests results (Figure 1). The average results obtained during PARTNER project for the accelerated mortar bar test RILEM AAR-2 with long prisms (40×40×160mm) [28] were used. These first results show a correlation between the size descriptors and the expansion test results, in agreement with previous results of [14, 15]. Work in progress is focus on the grain size analysis of quartz in more samples, including different rock types, and in the investigation of a correlation between other parameters, like grain shape. The deformation degree of the rock will be reflected in the shape of its quartz grains. As result of increasing deformation, the shape of quartz grains tends to be more irregular and elongated. Image analysis give us the unique opportunity of using the same sets of input images that are used to grain size analysis to subsequent investigation of grain shape. All the parameters will be compared against expansion test results in order to verify if there is a correlation between the different parameters and the reactivity of the aggregates.

The results of detailed petrography and XRD are consistent with each other. The mineral characterization by XRD was especially useful in the identification and quantification of silica polymorphs other than quartz. Combined trydimite and cristobalite content in D1-01 and D1-05 determined by XRD are consistent with the opaline silica content determined by petrography. When evaluating the results of XRD analysis it was of interest to compare the wt% of the different silica minerals with expansion tests results. In the PARTNER test program, short (40x40x160 mm) and long bars (25x25x285 mm) were used in RILEM

AAR-2 to compare the effect in the results obtained. For those aggregates where both coarse and fine fractions existed, the results of testing the crushed coarse fraction were compared with those of the fine fraction. Table 5 summarizes the results obtained during PARTNER project for the accelerated mortar bar test RILEM AAR-2 for the aggregates B1, D1, F1, and G1 [28]. The aggregate F1 has the higher wt% of quartz but the lowest expansion value. This can be explained by the fact that pure reactive siliceous aggregates such as flint/chert have a pessimum effect, as defined by Hobbs [29]. For a given level of alkalis, the expansion of concrete increases with the reactive aggregate content to reach a maximum value. For aggregate content superior to the maximum, the expansion decreases due to an excess of reactive silica. Concretes based on both coarse and fine aggregate of reactive flint/chert usually do not swell. A recent investigation by Garcia-Diaz *et al.* [30] with siliceous limestones concluded that contrary to the pure siliceous aggregates, the content of reactive silica in siliceous limestones is too low to consume a maximum of alkalis in non-expansive adsorption process and to obtain non-expansive concretes. This is in agreement with the results obtained for the aggregates B1 and G1. Both have variable amounts of carbonates and higher reactivity than the aggregate F1. The presence of silica polymorphs other then quartz, notably cristobalite and tridymite was detected in the two specimens of the aggregate D1 that were analyzed. Zhang [16]defend that the phase in which silica occurs plays the dominant role in determining the reactivity, with disordered structures more reactive than structures containing cristobalite, which are in turn more reactive than structures containing quartz.

5 CONCLUSIONS

Initial results from microstructural characterization by grain size analysis of quartz of a number of aggregates showed that rocks with higher grades of deformation have a larger total grain boundary area of quartz than rocks with less deformation. This is in agreement with the results of [14, 15]. Work in progress is focus on the grain size analysis of quartz in more samples, including different rock types, and in the investigation of a correlation between other parameters, like grain shape, in an attempt to understand better the influence of the microstructure of the so called slowly-reactive rock types in it ASR-reactivity.

First results from mineralogical characterization by XRD of several aggregates have shown that the dominant silica polymorph in the aggregate plays indeed a dominant role in determining it reactivity as defended by [16]. By investigating the presence of different silica polymorphs in more samples of flint/chert and siliceous limestone, the authors aim to understand better the heterogeneous behaviour of these rock types towards the ASR.

Future work shall also focus on the quality of the crystal lattice of quartz, the presence of foreign species in the solid silica, and the presence of hydrous species in the solid silica, since all these parameters can reflect a certain degree of deformation or distortion of the ideal crystallographic structure of quartz that will affect it solubility. A better knowledge of the properties and qualities of silica minerals that can contribute to it dissolution in ASR-environment is essential to improve the actual knowledge about the AAR mechanisms and the test methods used to evaluate the reactivity of the aggregates for concrete.

6 ACKNOWLEDGEMENTS

First author NC acknowledges financial support from the Portuguese Fundação para a Ciência e Tecnologia (FCT) through doctoral grant reference SFRH/BD/41810/2007.

7 REFERENCES

[1] Lindgard, J, Nixon, PJ, Borchers, I, Schouenborg, B, Wigum, BJ, Haugen, M, Akesson, U (2010): The EU "PARTNER" Project - European standard tests to prevent alkali reactions in aggregates: Final results and recommendations, Cement Concrete Res, 40 611-635.

[2] AAR-1, R (2003): Detection of potential alkali-reactivity of aggregates - Petrographic method, TC 191-ARP: Alkali-reactivity and prevention – Assessment, specification and diagnosis of alkali-reactivity, prepared by: Sims, I, Nixon, P, , Mater Struct, 36 480-496.

[3] Broekmans, MATM (2002): The alkali-silica reaction: mineralogical and geochemical aspects of some Dutch concretes and Norwegian mylonites, in, University of Utrecht, pp. pp144.

[4] Broekmans, MATM (2004): Structural properties of quartz and their potential role for ASR, Mater Charact, 53 129-140.

[5] Haugen, M, Lindgård, J, Åkesson, U, Schouenborg, B (2008): Experience from using the RILEM AAR-1 petrographic method among European petrographers – part of the PARTNER project, in: M. Broekmans, B. Wigum (Eds.) 13th International Conference on Alkali-Aggregate Reaction in Concrete (ICAAR), Trondheim, pp. 744-753.

[6] Nixon, P, Lindgård, J, Borchers, I, Wigum, B, Schouenborg, B (2008): The EU "PARTNER" project – European standard tests to prevent alkali reactions in aggregates - final results and recommendations, in: M. Broekmans, B. Wigum (Eds.) 13th International Conference on Alkali-Aggregate Reaction in Concrete (ICAAR), Trondheim, pp. 300-309.

[7] AAR-2, R (2000): Detection of potential alkali-reactivity of aggregates - the ultra accelerated mortar bar test, Mater Struct, 33 283-283.

[8] AAR-4.1, R (2011): Detection of potential alkali-reactivity of aggregates. 60ºC accelerated method for aggregate combinations using concrete prisms, Committee Document RILEM /TC ACS/11/06, in preparation for publication in Materials and Structures.

[9] Broekmans, M, Fernandes, I, Nixon, P (2009): A global petrographic atlas of alkali-silica reactive rock types: a brief review, in: B. Middendorf, A. Just, D. Klein, A. Glaubitt, J. Simon (Eds.) 12th Euroseminar on Microscopy Applied to Building Materials, Dortmund, pp. 39-50.

[10] Schouenborg, B, Åkesson, U., Lieberg, L. (2008): Precision trials can improve test methods for alkali aggregate reactions (AAR) - part of the PARTNER project, in: M.A.T.M. Broekmans, Wigum, B.J. (Ed.) 13th International Conference on Alkali-Aggregate Reactions in Concrete, Trondheim, pp. 1186-1195.

[11] AAR-3, R (2000): Detection of potential alkali-reactivity of aggregates: method for aggergate combination using concrete prisms, Mater Struct, 33 209-293.

[12] Deutscher Ausschuss für Stahlbeton, D (2001): Vorbeugende Maßnahmen gegen schädigende Alkalireaktion im Beton : Alkali-Richtlinie, in, Beuth, Berlin, (DAfStb-Richtlinie).

[13] Castro, N, Wigum, BJ, Broekmans, MATM (2011): Deleterious alkali-silica reaction in concrete: preliminary petrographical and microstructural characterisation of reacted and virgin materials from PARTNER project, in: A. Mauko, A. Kosec, T. Tinkara, N. Gartner (Eds.) 13th Euroseminar on Microscopy Applied to Building Materials, Ljubljana, pp. 10.

[14] Wigum, BJ (1995): Examination of microstructural features of Norwegian cataclastic rocks and their use for predicting alkali-reactivity in concrete, Eng Geol, 40 195-214.

[15] Wigum, BJ, Hagelia, P, Haugen, M, Broekmans, MATM (2000): Alkali aggregate reactivity of Norwegian aggregates assessed by quantitative petrography, in: M.A. Bérubé, Fournier, B., Durand, B. (Ed.) 11th International Conference on Alkali-Aggregate Reactions in Concrete, Québec, pp. 533-542.

[16] Zhang, X, Blackwell, BQ, Groves, GW (1990): The Microstructure of Reactive Aggregates, Brit Ceram Trans J, 89 89-92.

[17] Blum, AE, Yund, RA, Lasaga, AC (1990): The Effect of Dislocation Density on the Dissolution Rate of Quartz, Geochim Cosmochim Ac, 54 283-297.

[18] Association, DS (2002): Concrete testing - hardened concrete - production of fluorescence impregnated plane sections (in Danish). DS 423.39, in, pp. 8.

[19] Association, DS (2002): Concrete testing - hardened concrete - production of fluorescence-impregnated thin sections (in Danish) DS 423.40, in, pp. 12.

[20] Humphries, DW (1992): The preparation of thin sections of rocks, minerals and ceramics, Royal Microscopical Society, Oxford Science Publications.

[21] Castro, N, Wigum, BJ (2011): Grain size analysis of quartz in potentially alkali-reactive aggregates for concrete: a comparison between image analysis and point-counting., in: M.A.T.M. Broekmans (Ed.) 10th International Conference on Applied Mineralogy, Trondheim, pp. 103-110.

[22] Heilbronner, R (1999): Lazy Grain Boundaries, public domain macros for NIH Image, in, University of Basel, http://pages.unibas.ch/earth/micro/index.html.
[23] Heilbronner, R (2000): Automatic grain boundary detection and grain size analysis using polarization micrographs or orientation images, J Struct Geol, 22 969-981.
[24] Barrett, SD (2008): Image SXM, in, http://www.ImageSXM.org.uk.
[25] Heilbronner, R, Bruhn, D (1998): The influence of three-dimensional grain size distributions on the rheology of polyphase rocks, J Struct Geol, 20 695-705.
[26] Heilbronner, R (1998): Stripstar, public domain program for the calculation of 3-D grain size distributions from histograms of 2-D sections, in, University of Basel, http://pages.unibas.ch/earth/micro/index.html.
[27] Castro, N, Sorensen, BE, Broekmans, MATM (2011): Assessment of individual ASR-aggregate particles by XRD, in: M.A.T.M. Broekmans (Ed.) 10th International Conference on Applied Mineralogy (ICAM), Trondheim, pp. 95-102.
[28] Jensen, J (2006): PARTNER report No. 3.2 Experience from testing of the alkali reactivity of European aggregates according to the RILEM AAR-2 method, SINTEF.
[29] Hobbs, DW (1988): Alkali-silica reaction in concrete, Thomas Telford Ltd., London.
[30] Garcia-Diaz, E, Bulteel, D, Monnin, Y, Degrugilliers, P, Fasseu, P (2010): ASR pessimum behaviour of siliceous limestone aggregates, Cement Concrete Res, 40 546-549.
[31] Whitney, DL, Evans, BW (2010): Abbreviations for names of rock-forming minerals, Am Mineral, 95 185-187.

Table 1: Compositions of selected slowly reactive bulk aggregate materials from PARTNER, by optical petrography on post-mortem concrete prisms and/or matching virgin coarse aggregate. These materials have been assessed by automated image analysis in a separate procedure. Further explanation in text. Table adapted from [13].

sample	brief lithological description	observed ASR reactive
It2	polymict rounded river gravel, main constituent quartzite, minor gneiss and granite, traces of flint/chert, gabbro, eclogite	quartzite, gneiss
N4	polymict rounded moraine gravel/sand containing sand-/siltstone, cataclasite, quartzite, granite, gneiss, gabbro, basalt	cataclasite, sandstone, quartzite
N5	polymict rounded glaciofluvial gravel/sand, main constituent quartzite, minor rhyolite, granite, gneiss, sandstone	quartzite, rhyolite
material provenance: It=Italy, N=Norway		

Table 2: Compositions of selected normally reactive (F1: non-reactive) bulk aggregate materials from PARTNER, by optical petrography on post-mortem concrete prisms and/or matching virgin coarse aggregate. These materials have been assessed by XRD in a separate procedure. Further explanation in text. Table adapted from [13].

sample	brief lithological description	observed ASR reactive
B1	angular fragments of various types of siliceous limestone (mud-, wacke-, packstones) containing foraminifera.	siliceous limestone
D1	sub-rounded glaciofluvial gravel/sand, main constituents flint/chert and opaline limestone, minor greywacke, quartzite, granite, gneiss, and mafic rocks.	flint/chert, opaline limestone
G1	partly crushed, partly naturally rounded polymict river gravel, main constituents flint/chert and siliceous limestone, minor quartzite, sandstone, greywacke, granite, and mafic rocks.	flint/chert, siliceous limestone, sandstone
F1	polymict rounded river gravel, main constituent flint/chert, minor siliceous limestone, mudstone, and greywacke.	flint/chert
material provenance: B=Belgium, D=Denmark, F=France, G=Germany		

Table 3: Results from automated image analysis of quartz in selected PARTNER lithologies, with alkali-reactivity confirmed by post-mortem optical petrography on concrete prisms. Further explanation in text.

sample	total number of quartz grains analyzed	mean grain size, d_{50} (mm)	total grain boundary area ($m^2 \cdot cm^{-3}$)
It2	14095	0.10	0.031
N4	13061	0.22	0.015
N5	27606	0.16	0.017

Table 4: Mineral modal compositions of selected PARTNER aggregate lithologies with confirmed alkali-reactivity, by XRD on polished sections, in vol% (normalized). Mineral acronyms cf. [31]. Further explanation in text.

		mineral					
sample	lithology	Qz	Cal	Dol	Crs	Trd	SUM
B1-12	siliceous limestone	15	85	1	<LLD	<LLD	100
B1-13	siliceous limestone	16	81	3	<LLD	<LLD	100
D1-01	opaline limestone	36	43	<LLD	12	8	100
D1-05	opaline limestone	51	29	1	12	6	100
G1-26	flint/chert	77	21	<LLD	<LLD	<LLD	100
G1-29	siliceous limestone	79	20	<LLD	<LLD	<LLD	100
G1-31	flint/chert	69	31	<LLD	<LLD	<LLD	100
F1-40	flint/chert	99	1	<LLD	<LLD	<LLD	100
F1-41	flint/chert	96	1	1	<LLD	1	100
F1-43	flint/chert	97	1	1	<LLD	1	100

Table 5: Selected 14-day expansion data on bulk aggregate from PARTNER, cf. RILEM AAR-2 with short prisms, in %. Further explanation in text. Table adapted from [28].

sample	fraction	results (14 days)		S/L ratio	reported reactivity in the field
		short (40×40×160 mm)	long (25×25×285 mm)		
B1	F	0.20-0.28	0.42	0.47-0.67	high
D1	C	0.25	0.18	1.39	very high
	F	0.23	-	-	very high (pessimum effect)
G1	C	0.27–0.41	0.46	0.59–0.89	high
F1	C	0.03	0.01-0.06	0.5-3	low-moderate (pessimum)

C = coarse fraction (> 4mm); F = fine fraction (< 4mm)

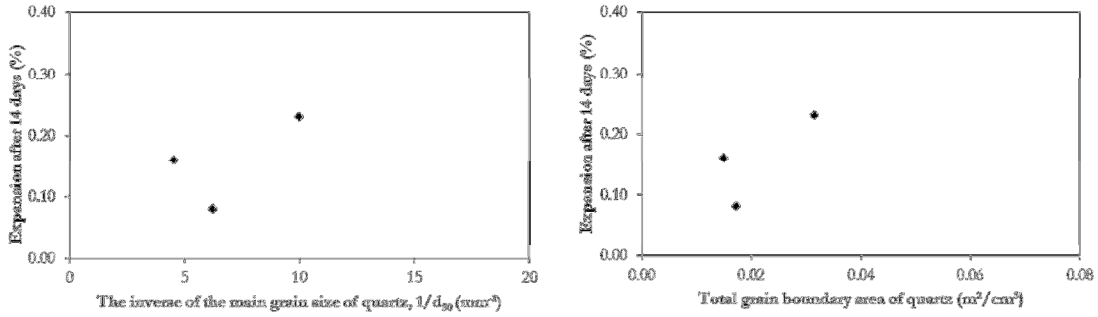

Figure 1: Correlation of average values of expansion data from PARTNER cf. RILEM AAR 2 on long prisms (%) [28], *versus* reciprocal quartz mean grain size 1/d50 (in mm^{-1}) at left, and *versus* total grain boundary area of quartz (in m^2/cm^3) at right.